THE BELL SYSTEM TECHNICAL JOURNAL
Vol. 62, No. 6, July–August 1983
Printed in U.S.A.

Modal Structure of an MCVD Optical Waveguide Fiber

By A. CARNEVALE* and U. C. PAEK†

(Manuscript received September 1, 1982)

In this paper we compare modal analyses of a Modified Chemical Vapor Deposition (MCVD) optical waveguide fiber and an idealized fiber. The pertinent profile parameters of the idealized fiber are obtained from the MCVD profile. We have validated the concept of an optimum α developed in our previous work. The reduction of the bandwidth of the MCVD fiber is shown to be directly related to the imperfections in the profile inherent in the MCVD manufacturing process.

I. INTRODUCTION

Multimode lightguides, produced by the Modified Chemical Vapor Deposition (MCVD) process, are expected to be of continuing importance to the Bell System. Such lightguides with bandwidths exceeding 1 GHz·km have been produced in the manufacturing plant.

The unique MCVD process produces the index gradient in the core by depositing many layers of material with different compositions, leading to a ripple effect in the profile. Other imperfections in the MCVD process include certain mechanical limitations, difficulties at the core-cladding interface, and the altering of the core center index (burn-off) during the collapse of the preform. These imperfections in the MCVD process lead to a unique modal structure in the fiber, which

* Bell Laboratories, Murray Hill, N.J. † Western Electric Company, Princeton, N.J.

may differ radically from the modal structure obtained from a perfect power law profile. These differences, for a particular fiber preform and idealization, are analyzed and compared. The effects of the imperfections on dispersion and bandwidth are evaluated.

II. EXPERIMENT

Our method[1] for solving Maxwell's equations has been described earlier and we shall not repeat it here. A brief schematic of the process is given in Fig. 1. In the experiment, the perfect power law profile (N_i)

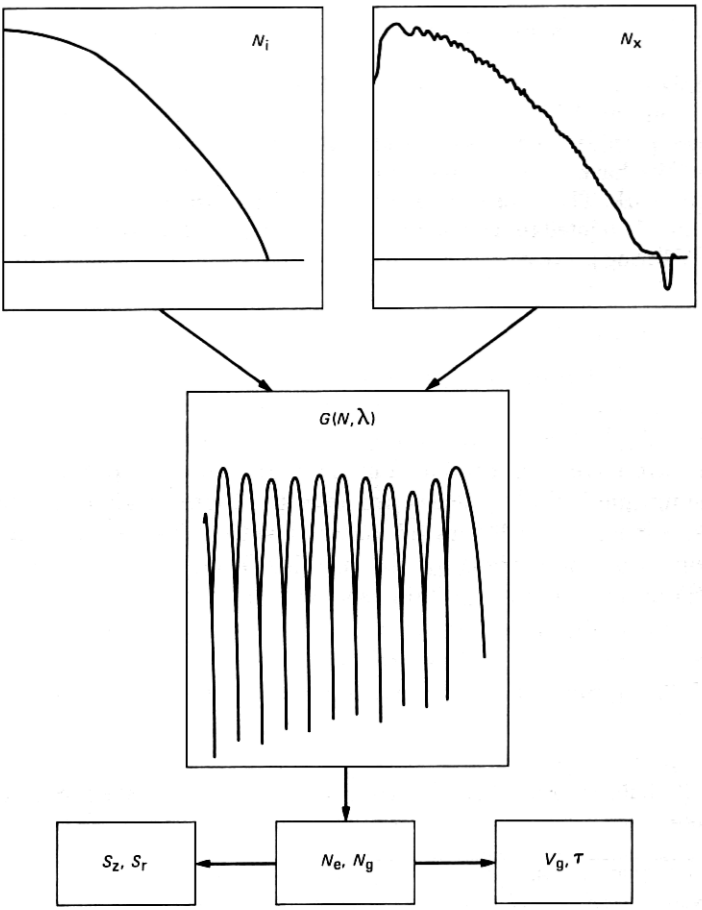

Fig. 1—N_i is a perfect power law profile. N_x is a typical MCVD profile that must be normalized in a particular way to be compatible with the calculations described in Ref. 1. From these calculations we obtain the G function, from which one further determines the effective indices, N_e, and the group indices, N_g. Further processing leads to the calculation of the Poynting vector, the field functions, the delay times, etc.

is replaced with the actual MCVD profile (N_x), which differs from the perfect profile. Thereafter, the data are processed identically to find the effective indices N_e, group indices N_g, the Poynting vector, and other propagation parameters.

An MCVD preform was given to us by S. Jang of the Western Electric Research Center in Princeton, N.J. This preform had been used earlier to produce fiber for experiments. It was typical in the sense that the bandwidths averaged 1 GHz·km. By means of the laser beam refraction method[2] the refractive index profile was determined and is shown in Fig. 2.

We note in this profile the familiar characteristics of the MCVD preform, i.e., a burn-off region in the center, an undefined core-cladding interface region, and ripples on the profile, which are more pronounced as we near the core center.

The pertinent data required for our analytical testing are the approximate $\bar{\alpha}$ and the maximum ΔN. These data can be obtained from known procedures,[2] or alternatively, as in our case, by utilization of the technique described in one of our earlier publications.[3] Briefly, at a selected wavelength, one obtains the modal display for zero azimuthal numbers, fits the data to a linear least squares equation for N_g vs. N_e,

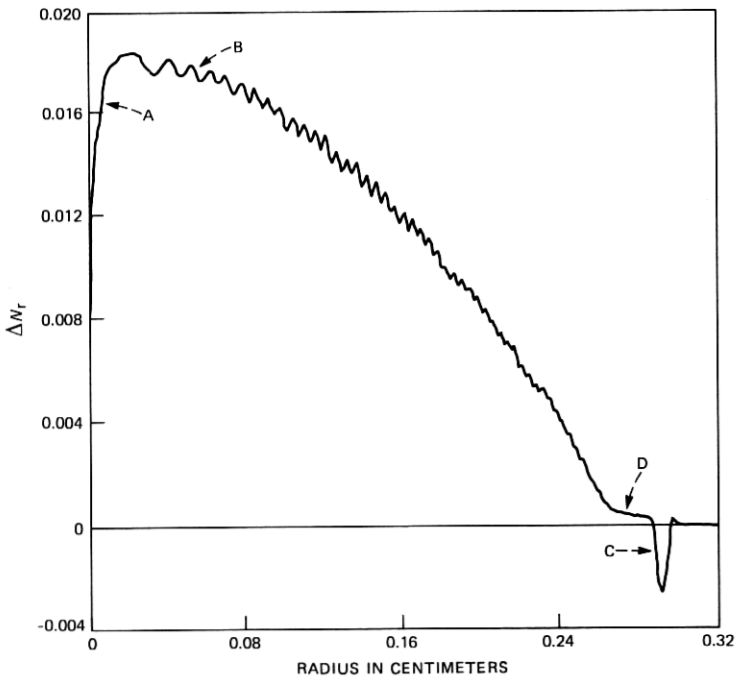

Fig. 2—Typical MCVD profile before normalization.

and compares this slope to the slope vs. α, which has been previously calculated for that wavelength. The parameters to be used in this case were $\alpha = 2$, ΔN is typical for an 11.5-percent GeO_2 dopant, and radius $(R_{cc}) = 25$ μm.

These data are then used to produce modal displays for perfect power law profiles (IDEAL) at the wavelengths and polar indices used for probing the experimental (MCVD) profile. The programs are run in parallel, to be used eventually for comparison purposes only, i.e., there is no communication between the two series of calculations.

Inherent in our calculations is the automatic detection of significant mode splitting between the EH vs. HE, or TE vs. TM, and in the displays to follow, the splittings are shown, wherever possible.

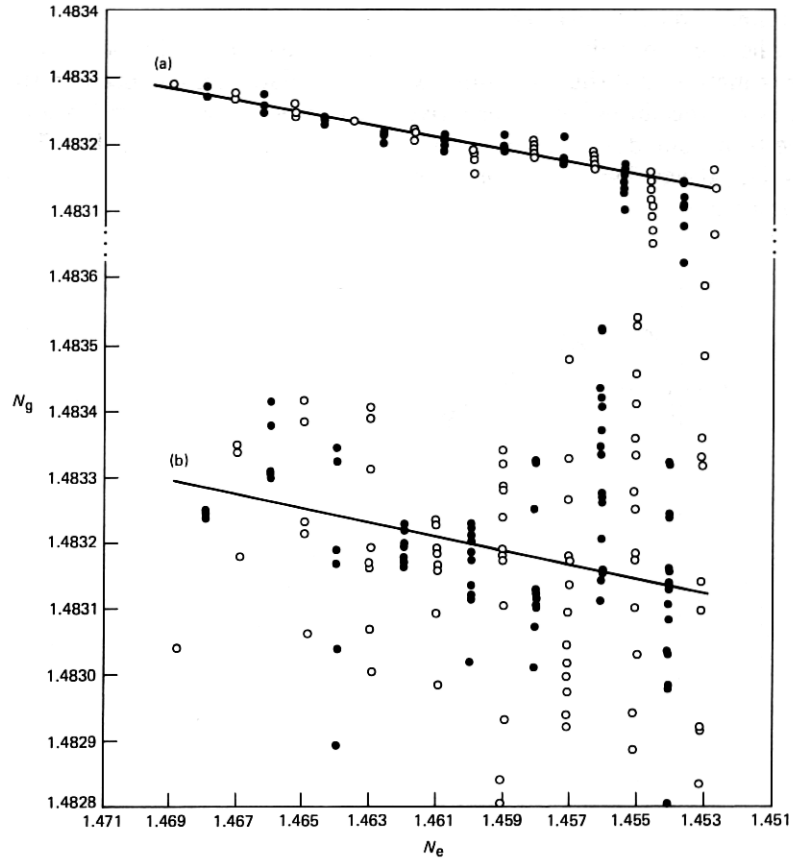

Fig. 3—Composite data for $\lambda = 0.9$ μm. The top portion (a) is the IDEAL. The bottom portion (b) is the MCVD. The straight lines are the linear least-squares curves fitted to all the data in each case, exclusive of those modes near the cladding, and for those modes widely divergent from the line. In general, the open circles are for polar indices $m = 1, 3, 5, \cdots$ last, while the solid circles are for polar indices $m = 0, 2, 4, \cdots$ last. Split modes are not readily identifiable in this display.

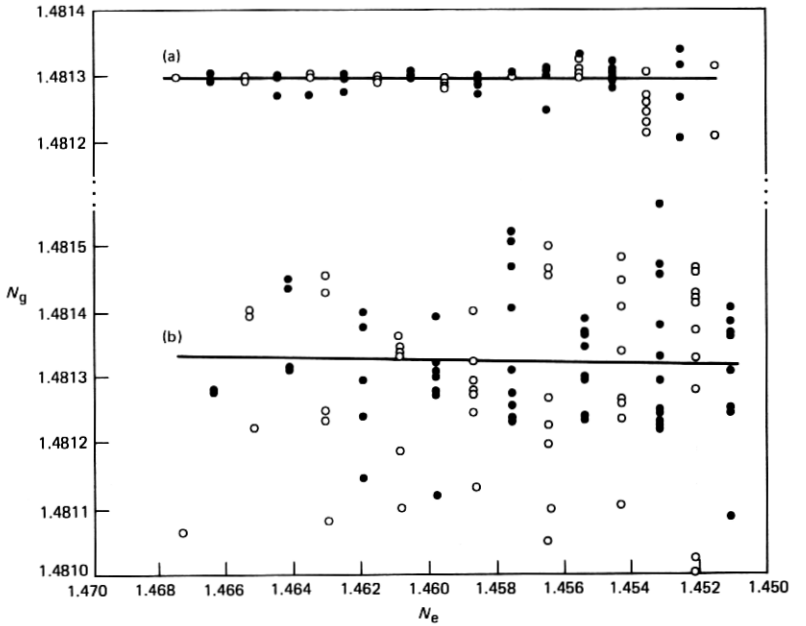

Fig. 4—Same as Fig. 3, $\lambda = 1.0\ \mu m$.

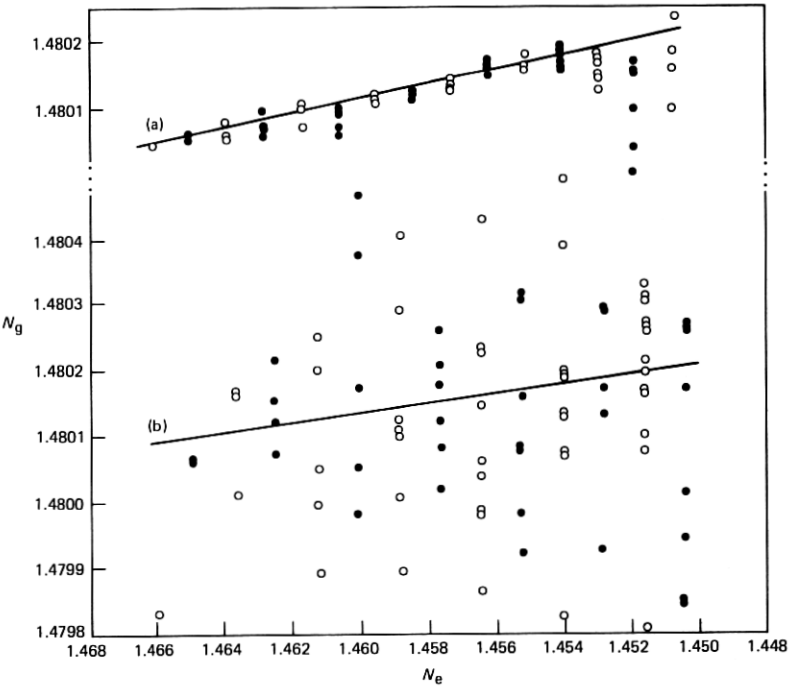

Fig. 5—Same as Fig. 3, $\lambda = 1.1\ \mu m$.

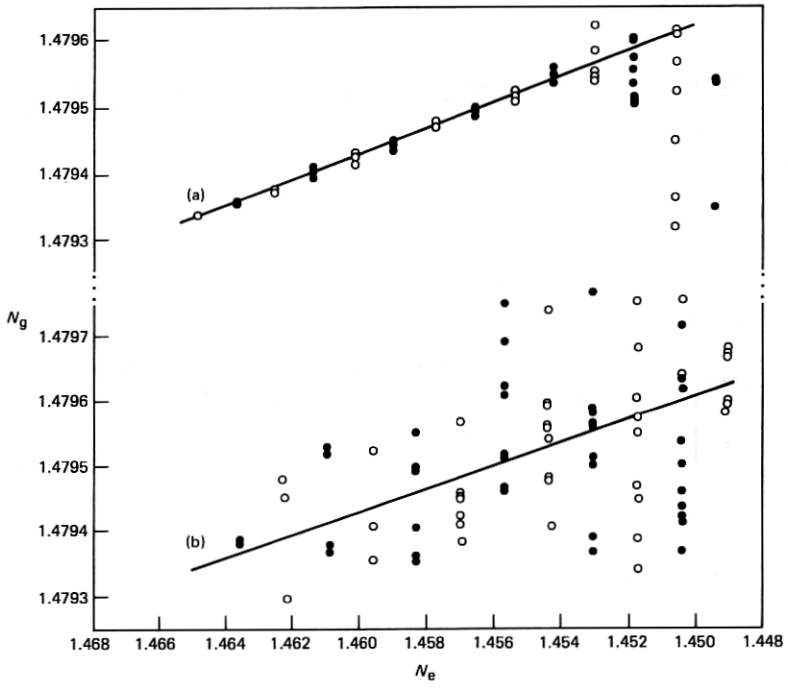

Fig. 6—Same as Fig. 3, $\lambda = 1.2$ μm.

We selected eight wavelengths (λ) spanning the region

$$0.9 \leq \lambda \leq 1.55 \ \mu\text{m}.$$

Each wavelength was checked for all possible modes ($m = 0, 1, 2, \cdots$ last) for both the IDEAL and the MCVD profiles. Because the extremely large amounts of data required in this analysis involved exorbitantly large amounts of computer time, we reduced the required accuracy to a minimum sufficient for our purposes, thereby saving considerable time and expense. Nevertheless, much computational time was required to accumulate the data given in this report.

Our results on the foregoing procedure are displayed in Figs. 3 through 10. In each figure, the dots represent the modes actually determined, the line is the linear least-squares curve fitted to the data, excluding some of the modes near cutoff, the upper portion (a) is for the IDEAL profile, and the lower portion (b) is for the MCVD profile. Again, some modes that are well off the chart are not shown because of space limitations and were not used to calculate the fitted curves in any case. All the fitted curves, translated where necessary but not rotated, have been condensed into the single plot given in Fig. 11.

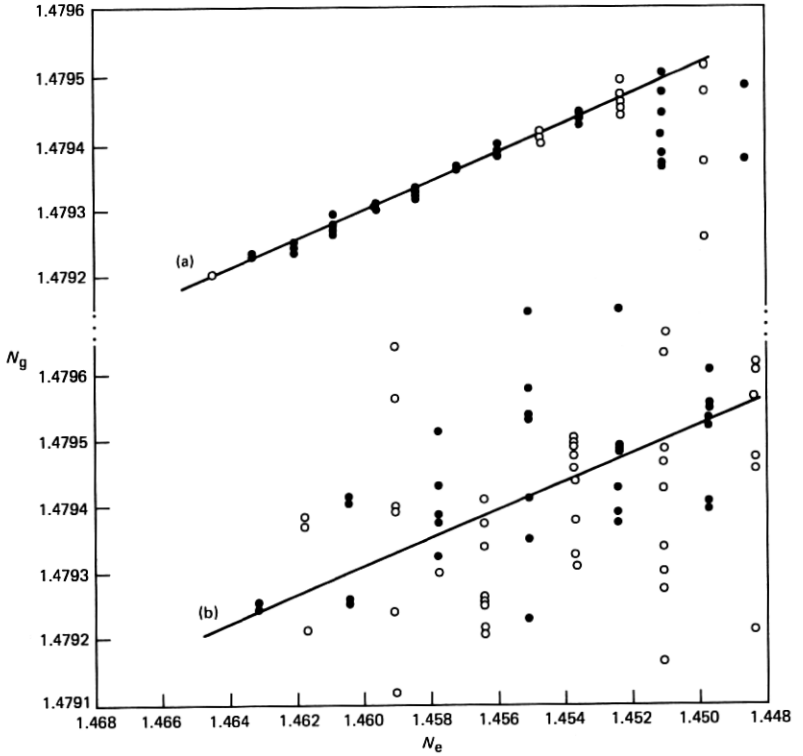

Fig. 7—Same as Fig. 3, $\lambda = 1.23$ μm.

III. DISCUSSION

The degree of scatter in the modes for the IDEAL case (Figs. 3 through 10, Part a) is due in part to the inherent splitting of the HE-EH modes, which has been further compounded by the reduced accuracy used in this analysis.

The scattering of the modes for the MCVD case (Figs. 3 through 10, Part b) is much greater than the IDEAL series, perhaps by a factor of 5 to 10. Obviously, the greatly increased scattering for the MCVD series is due to the imperfections in the MCVD profile, such as burn-off and ripple. The contribution of each of these imperfections to increased modal dispersion (poor bandwidth) has been determined and will be the topic of a forthcoming paper.

Further, within the statistical precision and accuracy employed by the authors, one can calculate that the IDEAL and MCVD data will both extrapolate to the same index at the core. We should realize that the MCVD index of refraction data of Fig. 2 was obtained at $\lambda = 0.6328$ μm. This must be converted to the proper ΔN at the probing

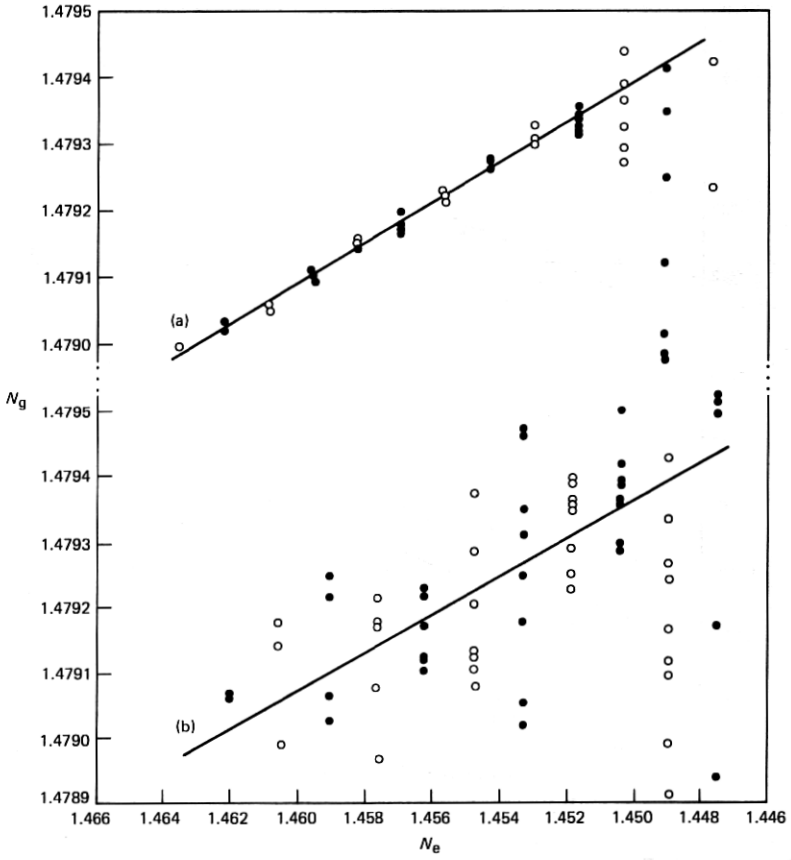

Fig. 8—Same as Fig. 3, $\lambda = 1.32$ μm.

λ's used in any analysis, and was done in this analysis. The results indicate that our parameter ΔN as calculated at each λ is reliable.

The parallelism of the least-squares fitted lines, seen in Fig. 11, indicates that our calculations of the parameter α from the MCVD profile are also reliable, and that an idealized profile may be used to predict characteristics of an MCVD profile. We must realize that α does not vary with λ, and this is true regardless of whether we are using the IDEAL or MCVD profile. We are immediately struck by the rotation of these curves as we change λ. We have noted a similar effect[3] at a fixed λ for a changing α. It should be noted that the previous work[3] and the present work agree closely.

We have one further observation in the present work, which is not readily seen in Figs. 3 through 10: although both the IDEAL and MCVD profiles were normalized to a 25-μm radius, the IDEAL profile

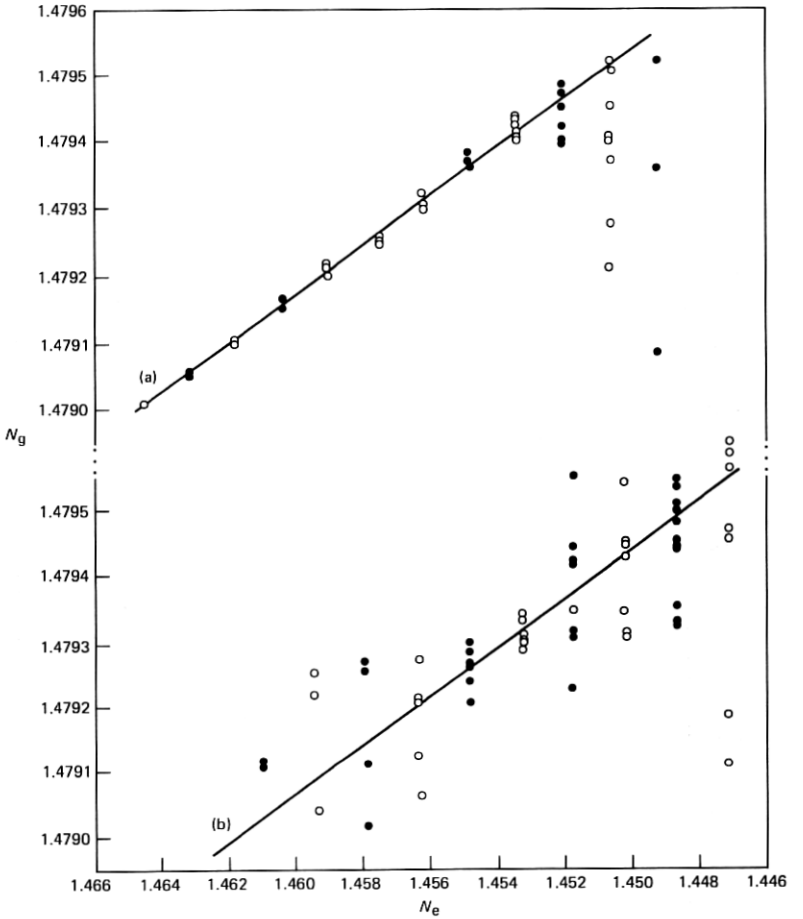

Fig. 9—Same as Fig. 3, $\lambda = 1.40$ μm.

generated more modes than the MCVD, without exception. To account for the fewer MCVD modes a crude estimation of the effective radius for the MCVD indicates that

$$r_e \approx 23 \ \mu\text{m}.$$

It may be only coincidence that this difference of 2 μm is of approximately the same magnitude as the width of the burnout.

IV. REDUCTION OF DATA

Two useful measures of dispersion were derived for this report. The first, which is relatively simple, is the calculation of the dispersion due to the rotation of the line as a function of λ. This implies that every

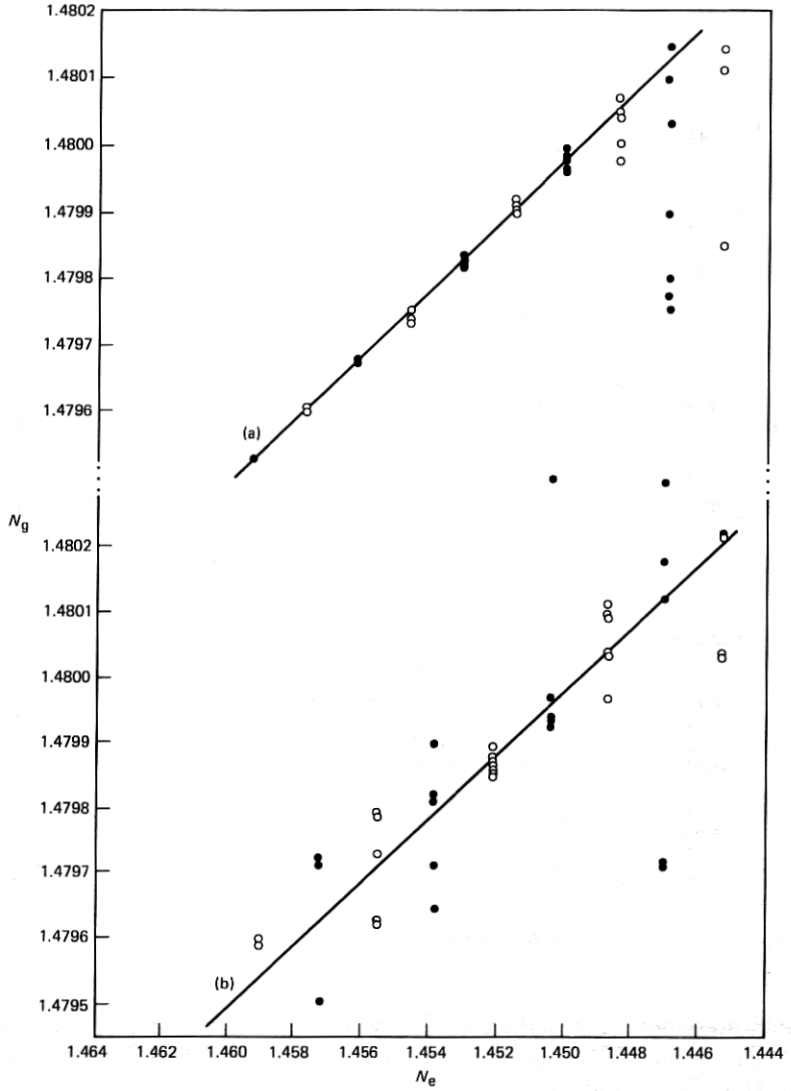

Fig. 10—Same as Fig. 3, $\lambda = 1.55$ μm.

group index (N_g) would be *on* the line. However, the total spread in N_g is now a function of the slope of the line, i.e., the spread in N_g between the $HE_{1,1}$ and the last possible mode that can be obtained on that line. We have given this measure the name "sigma of rotation", (σ_R). Of course, we must count the number of modes at each N_e to find the mean N_g and then calculate σ_R in the conventional manner.

The second measure of dispersion we have utilized is the standard deviation of the group indices determined from the indicated least-

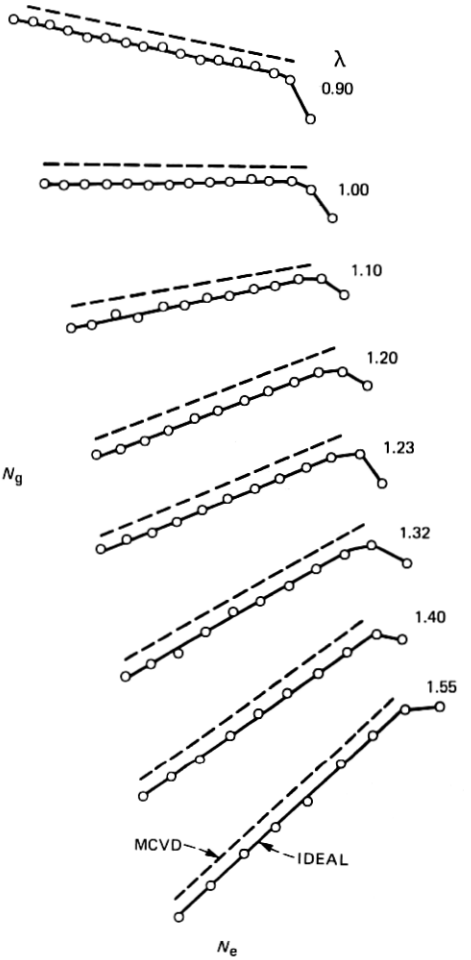

Fig. 11—Composite data. Least-squares fitted lines (IDEAL and MCVD) from the data of Figs. 3 through 10, identifiable in this display.

squares fitted line for N_g vs. N_e. Thus, if the curve value of N_g is denoted by $N_g(\text{curve})$, then

$$\sigma_{N_g} = \sqrt{\frac{\Sigma[N_g - N_g(\text{curve})]^2}{n-1}},$$

where n is the total number of modes.

The results of these calculations for σ_R are given in Fig. 12, and as indicated in Fig. 11, are about the same for the IDEAL and MCVD fibers. Further, if this were the only measure of dispersion employed,

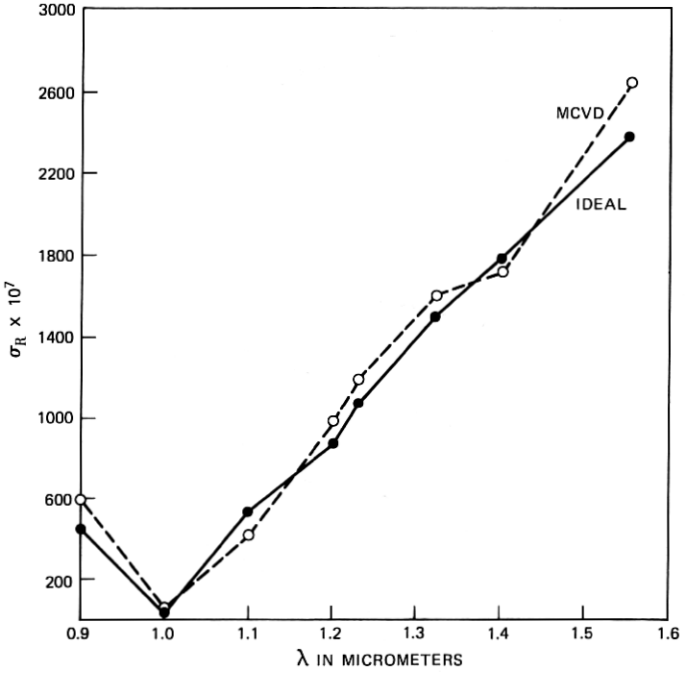

Fig. 12—σ_R vs. λ for IDEAL or MCVD.

we would expect this fiber to yield the maximum bandwidth at $\lambda = 1.00\ \mu m$. This agrees precisely with our previous work.[3] The results for the calculation of σ_{N_g} are given in Fig. 13 and we can see that:

$$\sigma_{N_g}(\text{MCVD}) \approx 10\ \sigma_{N_g}(\text{IDEAL}).$$

Also, we note further that σ_{N_g} is a decreasing function for larger values of λ, and becomes virtually constant when $\lambda \geq 1.2\ \mu m$.

A better understanding of the roles of the two measures of dispersion previously described is given in Figs. 14 and 15. In Fig. 14, σ_R and σ_{N_g} are plotted for the IDEAL case, and in Fig. 15 the same data are plotted for the MCVD case. Apparently, the σ that is dominant at any λ will be the principal cause of inability to maximize the bandwidth.

From theory[4] we have calculated the total dispersion σ_c by:

$$\sigma_c = \sqrt{\sigma_R^2 + \sigma_{N_g}^2},$$

and these data are given in Fig. 16. We see that in the region where σ_R is dominant ($\lambda \geq 1.2\ \mu m$), the curves are roughly parallel. The larger σ_c for the MCVD in this region comes about because the σ_{N_g} of the MCVD is greater than σ_{N_g} of the IDEAL.

Over the range $0.9\ \mu m \leq \lambda \leq 1.2\ \mu m$, the IDEAL case peaks ($\sigma_c =$

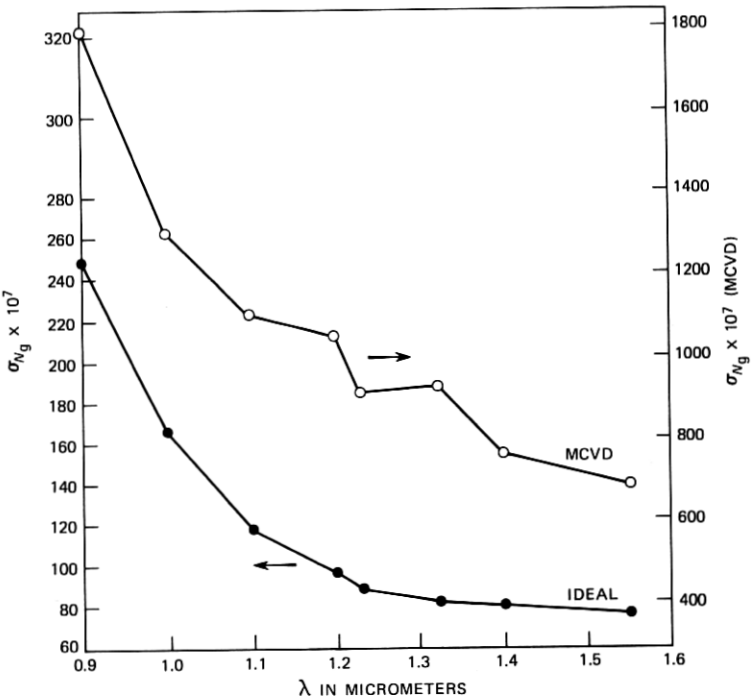

Fig. 13—σ_{N_g} vs. λ for IDEAL and MCVD.

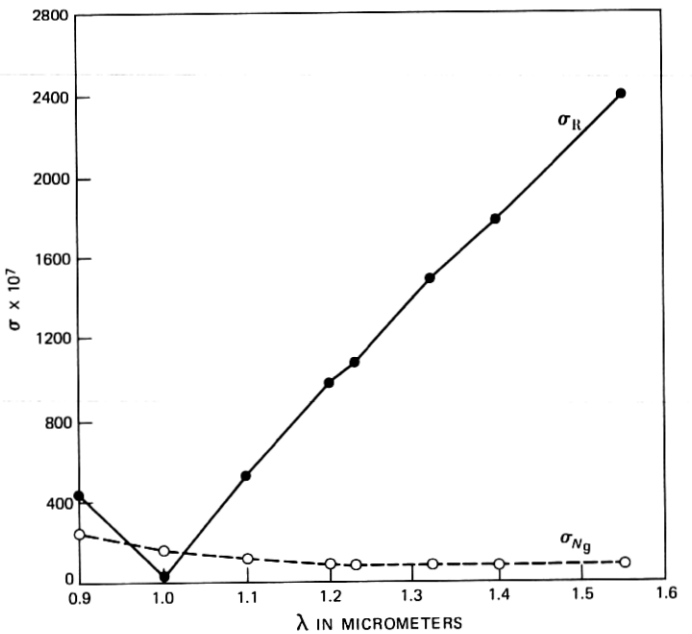

Fig. 14—(σ_R and σ_{N_g}) vs. λ for the IDEAL.

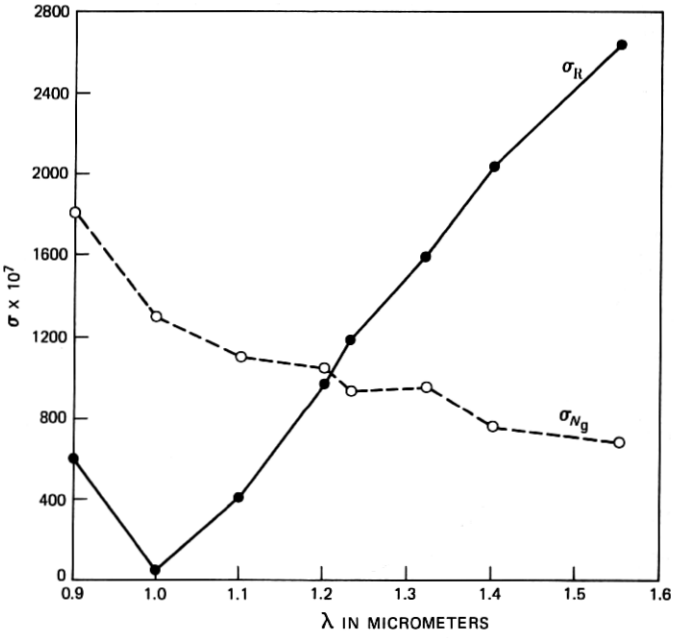

Fig. 15—(σ_R and σ_{N_g}) vs. λ for the MCVD.

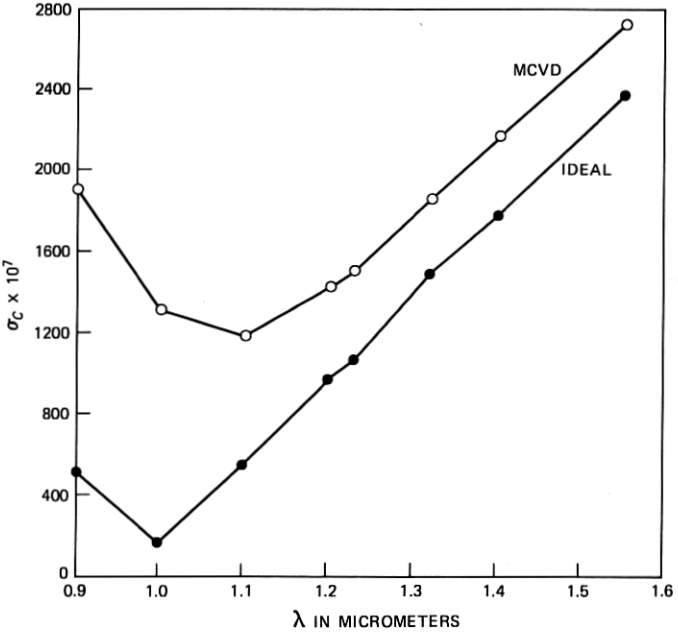

Fig. 16—σ_c vs. λ for IDEAL and MCVD.

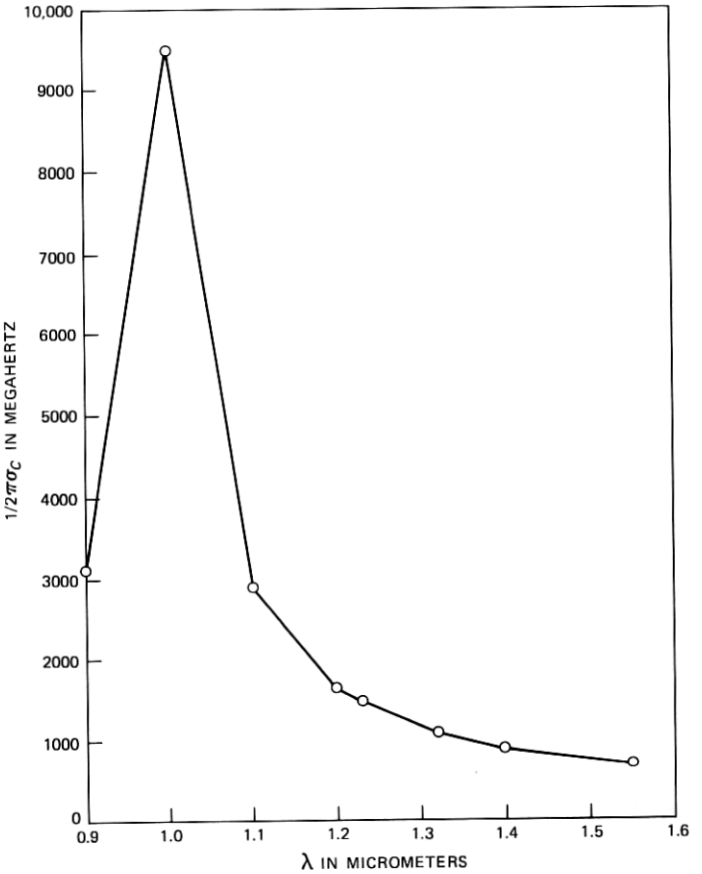

Fig. 17—$1/2\pi\sigma_c$ for the IDEAL case.

minimum) sharply at about 1.0 μm, while the MCVD displays a very broad response that appears to peak at about 1.1 μm. A qualitative measure to estimate the pulse shape can be realized by calculating $W(h/2)$; $W(h/2) = 1/2\pi\sigma_c$ (MHz).

These data are given in Figs. 17 and 18 for the IDEAL and the MCVD, respectively. The IDEAL gives a bandwidth of 9 to 10 GHz/km at 1.0 μm and falls off to half-height at ± 0.7 μm. The MCVD obtains a maximum of about 1.5 GHz·km at ≈ 1.1 μm, and falls off to half height at ± 0.2 μm.

V. CONCLUSION

There can be no doubt that the concept of an optimum α is valid for perfect power law and for experimental (manufactured) profiles.[3] The reduction of the bandwidth is directly related to the imperfections

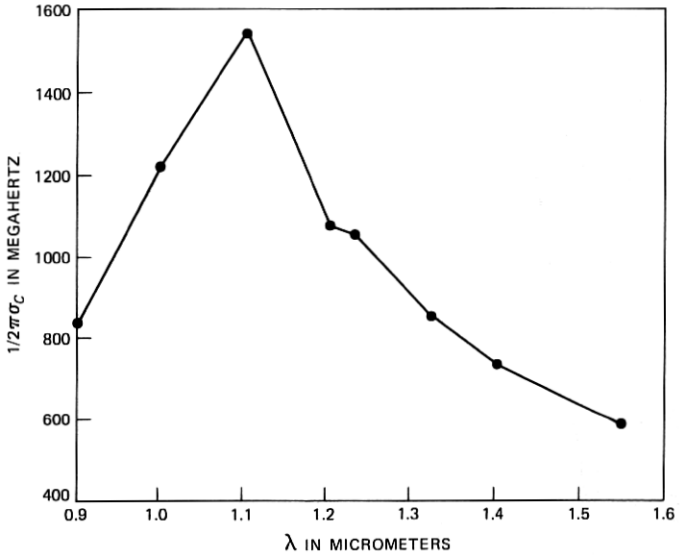

Fig. 18—$1/2\pi\sigma_c$ for the MCVD case.

of the MCVD profile such as burnout, ripples, etc. The direct role of each of these deviations from an idealized profile, in the reduction of bandwidth, has been calculated, and will be the subject of a forthcoming paper. These observations have been substantiated in many respects from direct communication with the materials scientists at Bell Laboratories in Murray Hill and Atlanta, and the Western Electric Company Engineering Research Center. We have also ascertained that we can improve the calculation of σ_{N_g} by about a factor of 2. Thus we find the bandwidth for the idealized fiber is about 18 GHz·km, while for the MCVD fiber it is about 2.8 GHz·km. These bandwidths can be further improved by careful computer-aided design of the profile, for which investigations are currently in progress.

VI. ACKNOWLEDGMENTS

We appreciate the continued support and encouragement given us in this work by M. I. Cohen, R. J. Klaiber, and L. S. Watkins. We are also encouraged by the enthusiasm of the materials scientists engaged in the lightguide program at Bell Laboratories in Murray Hill and Atlanta and Western Electric, as evidenced in a number of informal discussions with them.

REFERENCES

1. G. E. Peterson, A. Carnevale, U. C. Paek, and D. W. Berreman, "An Exact Numerical Solution to Maxwell's Equations for Lightguides," B.S.T.J., *59*, No. 7 (September 1980), pp. 1175–96.

2. L. S. Watkins, "Laser beam refraction traversely through a graded-index preform to determine refractive index ratio and gradient profile," Applied Optics, *18* (July 1, 1979), pp. 2214–22.
3. G. E. Peterson, A. Carnevale, U. C. Paek, and J. W. Fleming, "Numerical Calculation of Optimum α for a Germania-Doped Silica Lightguide," B.S.T.J., *60*, No. 4 (April 1981), pp. 455–70.
4. J. M. Wozencraft and I. M. Jacobs, *Principles of Communication Engineering*, New York, NY: John Wiley & Sons, p. 93.

AUTHORS

Un-Chul Paek, B.S. (Engineering), 1957, Korea Merchant Marine Academy, Korea; M.S., 1965, Ph.D., 1969, University of California, Berkeley; Western Electric, 1969—. At the Western Electric Engineering Research Center, Princeton, N.J., Mr. Paek has been engaged primarily in research on laser material interaction phenomena and fiber optics. Member, Optical Society of America, American Ceramic Society, Sigma Xi.

Anthony Carnevale, B.S. (Physics), 1960, Fairleigh Dickinson University; Bell Laboratories, 1969—. At Bell Laboratories, Mr. Carnevale has been engaged in research on nuclear magnetic resonance, electron paramagnetic resonance, and computer software. For the last four years, his work has been devoted to fiber optics.